



SPE 56476

Gas Condensate Relative Permeability for Well Calculations

Curtis H. Whitson/NTNU and Pera, Øivind Fevang/Pera, and Aud Sævareid/ResLab

Copyright 1999, Society of Petroleum Engineers, Inc.

This paper was prepared for presentation at the 1999 SPE Annual Technical Conference and Exhibition held in Houston, Texas, 3-6 October, 1999.

This paper was selected for presentation by an SPE Program Committee following review of information contained in an abstract submitted by the author(s). Contents of the paper, as presented, have not been reviewed by the Society of Petroleum Engineers and are subject to correction by the author(s). The material, as presented, does not necessarily reflect any position of the Society of Petroleum Engineers, its officers, or members. Papers presented at SPE meetings are subject to publication review by Editorial Committees of the Society of Petroleum Engineers. Electronic reproduction, distribution, or storage of any part of this paper for commercial purposes without the written consent of the Society of Petroleum Engineers is prohibited. Permission to reproduce in print is restricted to an abstract of not more than 300 words; illustrations may not be copied. The abstract must contain conspicuous acknowledgment of where and by whom the paper was presented. Write Librarian, SPE, P.O. Box 833836, Richardson, TX 75083-3836, U.S.A., fax 01-972-952-9435.

Abstract

This paper addresses several issues related to the modeling and experimental design of relative permeabilities used for simulating gas condensate well deliverability.

The key relation defining steady-state flow in gas condensate wells is k_{rg} as a function of k_{rg}/k_{ro} . Strictly speaking, saturations are not important – i.e. the determination of $k_r(S)$. Once the $k_{rg}=f(k_{rg}/k_{ro})$ relationship is experimentally established and correlated with capillary number (N_c), accurate modeling of condensate blockage is possible.

Special steady-state experimental procedures have been developed to measure k_{rg} as a function of k_{rg}/k_{ro} and N_c . Saturations, though they can be measured, are not necessary. We have paid particular attention to the effect of hysteresis on the relation $k_{rg}=f(k_{rg}/k_{ro})$, based on our observation that many repeated cycles of partial/complete imbibition and drainage occur in the near-well region during the life of a gas condensate well.

An approach for fitting steady-state gas condensate relative permeability data has been developed and used for modeling relative permeability curves. A generalized relative permeability model is applied, where the “immiscible” or “rock” curves are linked with “miscible” or “straight-line” curves by a *transition function* dependent on the capillary number.

Treatment of “inertial” high velocity flow (HVF) within the condensate blockage region *and* locally at the wellbore are also treated.

The composite effect of condensate blockage is handled using a “Muskat” pseudopressure model, where relative permeabilities are corrected for the positive effect of capillary number dependence and the negative effect of inertial high velocity flow.

Introduction

Relative permeability effects in gas condensate reservoirs can be classified into three categories: (1) near-well steady-state gas/oil flow where saturation hysteresis is severe throughout the life of a well – experiencing hundreds of cycles of complete or partial imbibition and drainage; (2) in the bulk of the reservoir far-removed from the wells, an imbibition process occurs throughout the life of the reservoir, where liquid mobility is (practically) zero and only gas flows at a somewhat reduced permeability; and (3) water encroachment, where gas and/or retrograde condensate are trapped in quantities from 15-40 saturation percent, and water permeability can be significantly reduced.

In terms of *reservoir well performance*, the near-well relative permeability behavior is the dominant factor. The far-removed region of condensate accumulation has somewhat reduced gas relative permeability, but this effect is generally a second-order or negligible effect. Trapped saturations and reduced water relative permeability can be important for reservoir performance, but has no direct effect on well performance prior to water breakthrough.

The purpose of this paper is to present an engineering approach to treating gas-oil relative permeabilities describing near-well flow in gas condensate wells. Our approach is founded on the fundamental flow behavior near and around gas condensate wells. This flow behavior is characterized by a condensate “blockage” near the wellbore where gas relative permeability is reduced by the buildup of a significant *mobile* condensate saturation. Condensate blockage may reduce well deliverability appreciably, though the severity depends on a number of reservoir and well parameters.

We concentrate on the steady-state flowing conditions found in the near-well region – typically 1 to 100 m away from the wellbore. Specifically, we try to use laboratory pressures and flow velocities (or capillary numbers) similar to those experienced by wells *in a given field*. Relative permeability measurements are limited to the key data required to model flow behavior at these conditions – namely the relationship $k_{rg}=f(k_{rg}/k_{ro})$.

The dependence of $k_{rg}=f(k_{rg}/k_{ro})$ on capillary number may also be important, particularly for rich condensates with high delivery pressures (i.e. high bottomhole flowing pressures when the well is on decline). Capillary number describes the

relative balance of viscous and capillary forces ($N_c = \Delta p_{\text{viscous}}/P_c$), where $N_c = v_{pg}\mu_g/\sigma_{go}$. For small N_c , capillary forces dominate and traditional (“immiscible”) relative permeability behavior is found. For large N_c viscous forces dominate and relative permeabilities tend to approach straight lines or “miscible-like” behavior.

As part of this study an experimental program was conducted to serve two main purposes: (1) developing a consistent and flexible apparatus for measuring steady-state gas-oil relative permeabilities for synthetic-model and reservoir fluid systems, and (2) studying the effect of varying flow conditions in a gas condensate well which impose large saturation changes and significant saturation hysteresis.

In our modeling approach, we correlate measured relative permeability data using a generalized equation that consists of a traditional “immiscible” (Corey-type^{5,21}) relation and a simple one-parameter correlation for capillary number dependence. Because the measured data are of the form $k_{rg} = f(k_{rg}/k_{ro})$ instead of $k_{rg}(S)$ and $k_{ro}(S)$, we do not require measurement of saturations. The immiscible correlations are transformed from their traditional format of $k_r(S)$ to $k_{rg}(k_{rg}/k_{ro})$ in the fitting process. Once the correlation is fit to measured data, it is readily converted back to the form $k_r(S)$ needed in traditional reservoir modeling. Scaling for the variation of endpoint saturations has also been addressed, where the approach is based on maintaining the fundamental relationship of $k_{rg} = f(k_{rg}/k_{ro})$.

The results of our experimental and modeling work on relative permeability has been implemented in full-field reservoir simulation models using the concept of a generalized pseudopressure function. Well productivity calculations based on pseudopressure include the effects of condensate blockage, capillary number dependence of relative permeability, high-velocity (“non-Darcy”) effects, and well geometry.

Background and Theory

Condensate blockage may reduce well deliverability appreciably, though the severity depends on a number of reservoir and well parameters. Condensate blockage is important if the pressure drop from the reservoir to the wellbore is a significant percentage of the total pressure drop from reservoir to delivery point (e.g. a surface separator) *at the time (and after) a well goes on decline*. Reservoirs with low-to-moderate permeability (<10-50 md) are often “problem” wells where condensate blockage must be handled properly. Wells with high kh products (>5-10,000 md-ft) are typically not affected by reservoir pressure drop because the well’s deliverability is constrained almost entirely by the tubing. In this case, condensate blockage is a *non-issue*.

Fevang and Whitson¹⁰ have shown that condensate blockage is dictated primarily by the relationship of $k_{rg} = f(k_{rg}/k_{ro})$. They show that the k_{rg}/k_{ro} ratio is given explicitly by PVT behavior,

$$k_{rg}/k_{ro} = (V_{ro}^{-1} - 1)(\mu_g/\mu_o) \dots\dots\dots (1)$$

where V_{ro} is the ratio of oil volume to total gas+oil volume of the mixture flowing into a well (produced wellstream), evaluated at pressures existing in the near-wellbore region. For example, a “rich” gas condensate at relatively moderate flowing near-wellbore pressures (100-200 bar) V_{ro} may be about 0.25. The μ_g/μ_o ratio is typically about 0.025/0.1 or about 0.25. This leads to a $k_{rg}/k_{ro} = (1/0.2 - 1)(0.25) = 1$ [the crossing point of the relative permeability curves]. As the reservoir depletes, the flowing wellstream becomes leaner and V_{ro} will decrease to a lower value – e.g. $V_{ro} = 0.025$. Interestingly, near-wellbore viscosities are more-or-less constant during depletion and the resulting late-life $k_{rg}/k_{ro} = (1/0.025 - 1)(0.25) = 10$.

This simple example illustrates the observation that the range of k_{rg}/k_{ro} experienced by a gas condensate well during its entire life of depletion will vary by only about one order of magnitude. The k_{rg} variation is even smaller – perhaps from 0.05 to 0.2 in this “rich” condensate example. Consequently, our approach to measuring relative permeabilities is to (1) determine the expected range of k_{rg}/k_{ro} spanned for a given reservoir from PVT properties of the gas condensate fluid system, then (2) concentrate on obtaining accurate k_{rg} data in this range of k_{rg}/k_{ro} . The measurements are preferably made at realistic flowing pressures and velocities.

Saturation measurements are, as mentioned earlier, not so important to the modeling of condensate blockage. Evinger and Muskat^{9,20} already made the same observation in 1942 for saturated oil well performance – where $k_{ro} = f(k_{rg}/k_{ro})$, independent of S_o . Still, we can not overemphasize the importance of this observation because it provides a more accurate and consistent interpretation of data from various sources (laboratories, model studies, etc.). A plot $k_{rg} = f(k_{rg}/k_{ro})$ – highlighting the relevant k_{rg}/k_{ro} range for the particular reservoir – provides a key tool for quantifying condensate blockage.

Hysteresis – Well Modeling Results

We have found that the changing saturation history in the near-well region of a gas condensate well is complex, as illustrated in Figs. 1-4. Repeated cycles of imbibition and drainage follow rate variations and shutin periods. Figs. 1-2 show the saturation history of a well at radii of 2.2 m and 3.5 m, where annual 12-hour shutins are imposed over a five-year period during depletion. Cycles of imbibition and drainage are repeated in association with each shutin. Similar cycles of hysteresis (not shown) also follow changes in production rate, and particularly abrupt reductions in rate.

Fig. 3 illustrates the complexity of saturation distribution around a well at the end of shutin periods. For the initial-test shutin, the *oil saturation* builds up from a pre-shutin value of 20-40% to S_o values at the end of the shutin of (a) 100% at $r < 2$ ft, (b) a critical fluid at 2 ft (0 or 100%), (c) 0-20% in the small interval $r = 8-10$ ft, and (d) 0% beyond 10 ft.

For subsequent shutins at 1, 2, and 5 years into depletion, the near-well region oil saturation increases from pre-shutin flowing saturations of about 55%, to end-shutin saturations of

100% near the well (3-20 ft), then monotonically decreases at increasing radii until the “average reservoir saturation” (due to retrograde condensation) is approached far into the reservoir.

Production following the shutin will cause a significant drainage of the built-up near-well saturations as shown in Figs. 1-2. This drainage behavior following shutins will be experienced with varying degree throughout the entire “condensate blockage” zone. This *drainage process* will continue indefinitely (at any given point in the blockage zone) until a new BHFP increase is imposed by rate reduction or shutin.

The near-well saturation hysteresis varies from reservoir to reservoir, but similar cycles of large saturation change is common to *all* gas condensates during the life of a well. We consider this behavior to constitute severe hysteresis, but hysteresis that can not readily be modeled. The hysteresis is neither strictly “imbibition” or strictly “drainage”, but a complex series of drainage-imbibition cycles. *The most important issue is whether the effect of such hysteresis has a large or small impact on k_{rg} .*

Hysteresis – Laboratory Results

We provide some experimental results that imply a minimal effect of hysteresis on the $k_{rg}=f(k_{rg}/k_{ro})$ relationship at low capillary numbers. **Fig. 5** shows a complete hysteresis test for one flowing mixture with $k_{rg}/k_{ro}=0.7$ conducted on a Berea core with a synthetic gas condensate. The initial flow period is at a constant gas rate of 30 cm³/min and constant core flowing pressure of 100 bar. The early-time increase in pressure drop corresponds with the build-up of the steady-state saturation distribution throughout the core, with decreasing effective gas relative permeability. After about 12 pore volumes injected (PV_{inj}), pressure drop stabilises at $k_{rg}=0.07$.

Velocity Hysteresis. The velocity hysteresis commences at about 32 PV_{inj}, with two decreasing rates of 18 and 9 cm³/min, return to base rate of 30 cm³/min, followed by two higher rates of 44 and 59 cm³/min. Each new rate was flowed for 1-5 PV_{inj}. Subsequent return to the base rate of 30 cm³/min required about 3 PV_{inj} before the original pressure drop (k_{rg} value) was again measured for another 2-3 PV_{inj}. The velocity test ends at about 49 PV_{inj}. For this particular velocity hysteresis test, no hysteresis was measured. For higher k_{rg}/k_{ro} values (lean mixtures), the velocity hysteresis tended to give slightly (5-10%) lower k_{rg} values than the original base value (which always was measured starting with a gas-filled core). For other 10-md North Sea sandstone tests, velocity hysteresis was found to be low by 5-20% of the base k_{rg} values, particularly for leaner mixtures.

Shutin/Drawdown Hysteresis. For the example hysteresis test in **Fig. 5**, a 12-hour shutin occurred following the velocity test (at about 49 PV_{inj}). Following the shutin period where core pressure remained at 375 bar, a single phase was assumed to have developed. During the subsequent flow test at base rate of 30 cm³/min and base core pressure of 100 bar, a short transient of high mobility is seen from the low-but-increasing pressure drop. After only about 2-3 PV_{inj} the base pressure drop ($k_{rg}=0.07$) was reached and maintained for about 7 PV_{inj}.

That is, no hysteresis was found in this test. Because saturations are not measured in our tests, it was uncertain whether the single-phase condition was oil or gas, though we estimated that a 100(1-S_{wi})% oil saturation develops for this rich mixture. Irregardless, a single phase definitely exists and either full imbibition or full drainage has occurred, followed by the re-establishment of the two-phase steady saturation condition. As described earlier and seen in **Figs. 1-3**, this type of change will be experienced (near-wellbore) hundreds of times during the life of a well.

In other hysteresis tests of this type for leaner mixtures (higher k_{rg}/k_{ro} values) and a low-permeability North Sea sandstone, the return to base rate and core flowing conditions yielded a slightly (10-20%) higher k_{rg} than the base “pre-hysteresis” value. We have found, as discussed below, that the final steady-state $k_{rg}=f(k_{rg}/k_{ro})$ relation is, for practical purposes, unaffected by the initial state of the core prior to starting a flow test. The initial core saturation prior to flow tests was varied in this study, ranging from initially gas saturated at S_{wi} to initially saturated at the final conditions from a previous flow test (with high steady-state flowing oil saturations ranging from 30-50%).

Flowing-Pressure Hysteresis. For the example hysteresis test in **Fig. 5**, a long-term three-point test was conducted from about 60-105 PV_{inj}. The first increase in core flowing pressure from 100 to 275 bar lasted almost 10 PV_{inj}. This was followed by an equally-long test with flowing pressure of 375 bar, and again by a 10-PV_{inj} test at 275 bar. Gas rate was constant at 30 cm³/min for all tests. Returning to the base core flowing pressure of 100 bar at about 93 PV_{inj} required some 2-3 PV_{inj} before stabilization. The final k_{rg} was the same as the base k_{rg} (pre-hysteresis) and remained so for about 10 PV_{inj} to the end of the test.

Other hysteresis tests of this type for leaner mixtures (higher k_{rg}/k_{ro} values) and a low-permeability North Sea sandstone, the return to base rate and core flowing conditions yielded a slightly (10-20%) higher k_{rg} than the base “pre-hysteresis” value.

Imbibition or Drainage – Neither ... Both

Considerable misunderstanding can be found in the literature regarding relative permeabilities in gas condensate wells, and particularly with respect to whether the process is “imbibition” or “drainage”. Most recently, Raghavan and Jones¹⁹ confuse the issue in the SPE Distinguished Author Series “Depletion Performance of Gas-Condensate Reservoirs”, where they write (our numbering):

“(1) Because the liquid phase is more wetting than the gas phase, the development of a liquid phase during depletion of a gas-condensate reservoir is considered to be an imbibition process. (2) Pressures around the wellbore, however, may become low enough for revaporization of the liquid to take place. (3) Thus, both drainage and imbibition relative permeability curves are needed for a complete understanding of the performance of gas-condensate reservoirs during depletion. (4) The depletion performance of a gas-condensate reservoir is, however, affected by the drainage process over

only a small volume of the reservoir near the well, and the time over which this occurs is relatively short. (5) In particular, all times during transient depletion and during fully-developed boundary-dominated flow are governed by an imbibition process.”

Contention (1) applies *only* in the far-removed region of the reservoir where condensate is continuously accumulating and oil saturation is continuously increasing. By definition, this is in an “imbibition” process. As discussed earlier, however, the relative permeability behavior in this “accumulation” region has only a second-order or negligible effect on well performance.

Contention (2) has never been shown, not in Jones-Raghavan publications¹⁶⁻¹⁸ or other publications that we are aware of. We have conducted detailed well simulations using a compositional model and multiple C_{7+} fractions, with flowing BHP as low as 250 psia, without ever having observed that oil saturation near the wellbore “vaporizes” to a zero (or low) saturation where oil has zero mobility. In fact, steady-state flow theory proves that as long as the BHFP is greater than the lower dewpoint of the produced wellstream, then $V_{ro} > 0$ and $k_{rg}/k_{ro} < \infty$, which guarantees two-phase gas/oil flow with both gas and oil saturations greater than zero.

Contention (3) concludes with a correct statement, but for the wrong reason. The multiple imbibition and drainage cycles actually experienced in the near-well region of a gas condensate well is not due to the vaporization effect mentioned in their second contention, but mainly because of rate changes and shutin periods that cause complete and partial cycles of imbibition and drainage. Even for the over-simplified case of a well producing at a constant BHFP at all times, the oil saturation at the wellbore will increase initially (“imbibition”), reach a maximum, and then decrease (“drainage”) during the remaining life of the well; the decrease in saturation is not due to revaporization, but because the flowing mixture (produced wellstream) is getting leaner.

Contention (4) is completely wrong. First of all, for the simple case of a well producing against a constant BHFP, the initial oil saturation increase – “imbibition” – is always followed by an *extended* period of oil saturation decrease – “drainage”. The drainage process is caused by the flowing mixture in the near-well region becoming leaner. The leaner mixtures must have increasing k_{rg}/k_{ro} values. For higher k_{rg}/k_{ro} values (at a given pressure), k_{rg} must be increasing. This implies a decreasing oil saturation, which is a drainage process. For this simplified case, it is the *drainage process* that describes the entire “blockage” region throughout most of the life of the reservoir.

In reality, the rate changes and shutin periods associated with normal (erratic) production behavior of actual gas condensate wells will lead to a much more complex saturation history that described above.

Contention (5) is wrong for the same reasons that contention (4) is wrong.

In conclusion, in the near-well region where condensate blockage occurs, practically unlimited cycles of drainage and imbibition hysteresis occur during shutins, rate changes, and

by the continuous depletion process. What one “calls” the process of saturation change in a gas condensate well is of no importance. The only issue is whether the cycles of saturation change have a quantitative impact on the relative permeability behavior [of $k_{rg}=f(k_{rg}/k_{ro})$], and if so, how they should be modeled.

Experimental Procedures

A closed-loop system²⁰ was built to measure steady-state relative permeabilities specifically for gas condensates. The closed-loop equipment was designed to satisfy the key requirements for steady-state flow near and around a well – namely, (1) define the $k_{rg}=f(k_{rg}/k_{ro})$ relation, where values of k_{rg}/k_{ro} are pre-calculated for a given reservoir based on oil relative volumes and viscosities measured “online” or modeled with an equation-of-state (EOS); (2) reach steady-state flowing conditions automatically using large pore volumes injected; and (3) allow measurements at practically any pressure below the dewpoint (i.e. with low to realistic IFTs) and for a large range of rates (pore gas velocities) from 10 to 100 mL/min (10^2 - 10^3 m/d pore velocity) using external Quizix pumps or 100-1000 mL/min (10^3 - 10^4 m/d pore velocity) using the system’s gas booster pump.

A large container houses an equilibrium gas/oil mixture with 30-50% equilibrium “reservoir” oil by volume. This “reservoir” container is held at a high pressure that provides an equilibrium dew-point gas which represents the mixture flowing throughout the near-well region. By varying the pressure of the “reservoir” container, the flowing mixture is varied from the initial (richest) fluid to leaner fluids representative of what will be produced later in depletion.

The equilibrium gas is pumped from the reservoir container through a back-pressure regulator to the pre-defined core pressure. The resulting two-phase mixture flows through the core and pressure drop is monitored versus time. Steady-state conditions are assumed when pressure drop stabilizes for at least 10 pore volumes injected, though several hundred pore volumes may typically be used.

The gas booster pump increases the pressure of the produced mixture from core outflow pressure to “reservoir” pressure. Having an equilibrium oil/gas system in the reservoir container ensures automatic re-equilibration of the produced mixture – this effluent mixture may be depleted of some heavier components while the core is building up to its steady-state oil saturation, or it may contain an excess of heavier components when the core oil saturation decreases from one steady-state condition to another, but re-equilibration is guaranteed.

It is possible to measure liquid dropout of the flowing mixture any time during the experiment using a visual PVT cell connected to the reservoir container. We estimate the potential dead-volume error to be less than 0.1% (1 cc of 1000 cc), and maximum error in visual reading of the liquid volume to be 1% (10 cc), with an “average” V_{ro} uncertainty of $\pm 10\%$. **Fig. 7** shows the sensitivity of calculated k_{rg}/k_{ro} to the oil relative volume.

A capillary viscometer is placed in-line parallel to the core holder. By inverting the reservoir container and lowering its pressure, the “reservoir” oil viscosity can be measured at the core pressure. This oil viscosity is not the same as the flowing oil viscosity condensed from the reservoir gas. We simply use the measured “reservoir” oil viscosity to tune the viscosity correlation which is then used to calculate the flowing oil viscosity.

The rates of gas and oil q_g and q_o flowing through the core are computed from the reservoir injection (pump) rate q_{gR} and PVT relations V_{π} and V_{ro} . V_{π} represents the ratio of total gas and oil volume at core pressure to the volume of single-phase gas mixture at reservoir pressure. V_{ro} represents the ratio of oil volume to the total gas+oil volume at core pressure. Consequently, $q_o = q_{gR} (V_{ro}/V_{\pi})$ and $q_g = q_{gR} ((1-V_{ro})/V_{\pi})$.

Relative permeabilities k_{rg} and k_{ro} are computed from the pressure drop Δp across the core of area A , gas and oil rates q_g and q_o , and viscosities μ_g and μ_o , $k_{rg} = q_g \mu_g L / (kA \Delta p)$ and $k_{ro} = q_o \mu_o L / (kA \Delta p)$.

In-situ saturations in the core are not usually measured, as we have previously shown that only the relation $k_{rg} = f(k_{rg}/k_{ro})$ is important. However, because the $k_{rg}(S)$ relation may have a second-order effect for richer gas condensates, a procedure for measuring saturations has been developed.

Fig. 6 shows some of our measured data on two (140-md) Berea cores and a (10-md) North Sea sandstone core. Also shown are measurements reported by Ham and Eilerts¹¹ for a (100-md) Berea core using a low-pressure N_2 -condensate fluid system.

The most important laboratory measurements are stable pressure drop, oil relative volume V_{ro} and oil viscosity μ_o . V_{π} and gas viscosity are usually known accurately, independent of the fluid system. V_{ro} and μ_o , however, may be difficult to predict accurately with PVT models, so we recommend direct measurement of these quantities – particularly oil viscosity.

Core pressure is selected to represent flowing conditions near the wellbore when wells go on decline – i.e. near minimum bottomhole flowing pressure. In most of our studies, $p_{core} = 100$ bar has been used. In general, the minimum BHFP will range from 100 to 250 bar. Unless we are studying capillary number dependence of the $k_{rg} = f(k_{rg}/k_{ro})$ relation, all flow tests are conducted at the same core pressure.

For tests measuring capillary number dependence of the $k_{rg} = f(k_{rg}/k_{ro})$ relation, we raise the core pressure to lower the gas-oil IFT (down to 0.1-1 mN/m), and use the booster pump to achieve high pore gas velocities (up to 10^4 m/d). The maximum capillary number obtainable is about 10^{-2} . Such N_c values are considerably higher than would ever be found in the near-well region when a well is on decline, but they might occur during well tests at higher BHFPs.

Immiscible Relative Permeability Models

We have found three relative permeability correlations useful for describing low-capillary number “immiscible” behavior of steady-state data measured for gas condensate cores.

Corey^{5,21}

$$k_{rg} = k_{rg}^o \left[\frac{(1-S_{oe})(1-S_{wi}) + S_m - 1}{S_m - S_{wi}} \right]^2 \left[1 - S_{oe}^{\left(\frac{\lambda+2}{\lambda}\right)} \right] \dots (2)$$

$$k_{ro} = k_{ro}^o \left[\frac{S_{oe} \cdot (1-S_{wi}) - S_{oc}}{1-S_{wi} - S_{oc}} \right] \cdot S_{oe}^{\left(\frac{\lambda+2}{\lambda}\right)} \dots (3)$$

where

$$S_{oe} \equiv \frac{S_o}{1-S_{wi}} \dots (4)$$

Chierici⁷

$$k_{rg} = k_{rg}^o \cdot \exp(-B \cdot R_g^{-M}) \dots (5)$$

$$k_{ro} = k_{ro}^o \cdot \exp(-A \cdot R_o^L) \dots (6)$$

where

$$R_g = \frac{S_g - S_{gc}}{1-S_{wi} - S_g} \quad (S_g > S_{gc}) \dots (7)$$

$$R_o = \frac{S_g}{1-S_{wi} - S_{oc} - S_g} \dots (8)$$

Arco¹⁵

$$k_{rg} = k_{rg}^o (1+c_{g2}) \cdot S_{ge}^{c_{g1}} \cdot \left(1+c_{g2} \cdot S_{ge}^{c_{g3}} \right)^{-1} \dots (9)$$

$$c_{g3} = c_{g1} \cdot \left(1 + \frac{1}{c_{g2}} \right) \dots (10)$$

$$S_{ge} \equiv \frac{S_g - S_{gc}}{1-S_{wi} - S_{gc}} \dots (11)$$

$$k_{ro} = k_{ro}^o (1+c_{o2}) \cdot S_{oe}^{c_{o1}} \cdot \left(1+c_{o2} \cdot S_{oe}^{c_{o3}} \right)^{-1} \dots (12)$$

$$c_{o3} = c_{o1} \cdot \left(1 + \frac{1}{c_{o2}} \right) \dots (13)$$

$$S_{oe} \equiv \frac{1-S_g - S_{wi} - S_{oc}}{1-S_{wi} - S_{oc}} \dots (14)$$

We generally use one of these three correlations to fit data in the form $k_{rg} = f(k_{rg}/k_{ro})$ – i.e. without the need for measured saturations. It is important to realize that the three correlations can usually describe similar $k_{rg} = f(k_{rg}/k_{ro})$ behavior but with

somewhat different $k_r(S)$ behavior. This is illustrated in **Figs. 8-10**. Fig. 8 shows the more-or-less same $k_{rg}=f(k_{rg}/k_{ro})$ behavior for the entire range of k_{rg}/k_{ro} of interest to gas condensate wells (0.1 – 100). **Fig. 9** shows the $k_r(S)$ curves on a semi-log plot, enclosing with a box the area of interest where k_{rg}/k_{ro} ranges from 0.1 to 100.

Fig. 10 shows the $k_r(S)$ curves on a cartesian plot, enclosing with a box the area of interest (to some rich gas condensates) where $k_{rg}(S)$ may have a second-order effect on pressure loss calculations in the “accumulation” region away from the well (Region 2 in the Fevang-Whitson paper¹⁰). If saturation measurements are made, they should be made in this region. These S_o data are used together with the $k_{rg}=f(k_{rg}/k_{ro})$ data in fitting the relative permeability correlation.

Capillary Number Dependence

We propose a generalized relative permeability model, where the “immiscible” or “rock” curves are linked with “miscible” or “straight-line” curves through a transition function dependent on capillary number, $f_I(N_c)$. The transition function is a smooth and continuous relation without a “threshold” N_c value.

For low capillary numbers, the immiscible curves apply and $f_I=1$. For sufficiently high capillary numbers the miscible curves apply and $f_I=0$. A constant k_{rg}/k_{ro} value (instead of saturation) defines the immiscible and miscible relative permeability values used in the generalized correlation.

The immiscible relative permeability models contain a number of (2-10) adjustable parameters, while the transition function f_I has only two adjustable parameters. Non-linear regression locates the minimum (weighted sum-of-squares) deviation between measured and model k_{rg} data for a given set of measurements with varying k_{rg}/k_{ro} and N_c values. (Table 1).

Proposed N_c Model Dependence

Capillary number is defined as the ratio of viscous forces to capillary retaining forces

$$N_c = \frac{\Delta P_v}{P_c} \dots\dots\dots (15)$$

Capillary number has often been expressed by the approximate relation

$$N_c \cong N_{cg} = \frac{v_{pg} \cdot \mu_g}{\sigma_{go}} \dots\dots\dots (16)$$

$$v_{pg} = \frac{v_g}{\phi \cdot (1 - S_{wi})} \dots\dots\dots (17)$$

where v_{pg} is a “pore” gas velocity and v_g is Darcy gas velocity. As discussed in the Appendix, a more rigorous capillary number can be defined, without having an impact on the proposed methods given in this section.

Relative permeability of gas including capillary number dependence is given by²³

$$k_{rg} = f_I \cdot k_{rgI} + (1 - f_I) \cdot k_{rgM} \dots\dots\dots (18)$$

where k_{rgI} is the immiscible ($N_c=0, f_I=1$) gas relative permeability, and k_{rgM} is the miscible ($N_c=\infty, f_I=0$) straight line gas relative permeability

$$k_{rgM} = k_{rg}^o \cdot \frac{1}{1 + (k_{rg} / k_{ro})^{-1}} \dots\dots\dots (19)$$

Our application of Eq. 18 is different than others^{3-4,8} because we evaluate k_{rgI} and k_{rgM} at the same value of k_{rg}/k_{ro} – not at the same saturation. The limit to our approach is that it only can be used for the steady-state region where both gas and oil are flowing. The advantage is that only one set of parameters are required for correlating f_I data, not four potentially separate sets for k_{rg}, k_{ro}, S_{gc} , and S_{oc} .

We propose that the term f_I be given by

$$f_I = \frac{1}{(\alpha \cdot N_c)^n + 1} \dots\dots\dots (20)$$

where

$$\alpha = \frac{\alpha^o}{k_{rg}} ; \bar{k}_{rg} = \frac{k_{rgM} + k_{rgI}}{2} \dots\dots\dots (21)$$

α^o is a constant dependent only on rock properties. Based on regression of Heriot-Watt¹²⁻¹³ and Delft^{2,4} $k_{rg}=f(k_{rg}/k_{ro})$ data, we found a good estimate for α^o given by

$$\alpha^o = \frac{10^4}{\sqrt{k\phi}} \dots\dots\dots (22)$$

where k is absolute permeability in md and ϕ is porosity (fraction). Exponent n was an empirical constant found to equal 0.65 for several published data sets using the approximate gas capillary number definition N_{cg} .

If saturation is used to link k_{rgI} to k_{rgM} and k_{roI} to k_{roM} , then separate parameters (n_g, α_g) and (n_o, α_o) are apparently needed for each phase. Experimental evidence by Blom and Hagoort⁴ suggest that $n_g < n_o, n_g \approx 1$ and $n_o \approx 1-3$ using saturation to link k_{rI} and k_{rM} ; also, $\alpha_g/\alpha_o = 1-100$. **Fig. 11** shows the behavior of f_I versus αN_c for $n=0.75, 1, \text{ and } 3$.

Furthermore, with saturation as the “linking” variable, critical saturations S_{oc} and S_{gc} must also be correlated from immiscible to miscible values using additional sets of parameters (n_{Sgc}, α_{Sgc}) and (n_{Soc}, α_{Soc}). Clearly, the price for a more general treatment of capillary number dependence is additional complexity. Our experience is that the complexity is neither necessary or justified to match steady state gas-oil relative permeabilities needed in well calculations.

Designing the Relative Permeability Data

Our recommendation for measuring relative permeability data used in well modeling of gas condensate reservoirs is outlined below.

Defining Range of Relevant k_{rg}/k_{ro}

We recommend that, as a minimum, five *immiscible* k_{rg} data be measured for a specific range of k_{rg}/k_{ro} values. These k_{rg}/k_{ro} values are those which dominate flow in the condensate blockage region near the well, and they are defined *only by PVT properties* of the fluid system (Eq. 1).

First, a constant-volume depletion (CVD) experiment is simulated. For each CVD gas removed, a constant-composition experiment (CCE) is simulated, reporting $V_{ro}=V_o/V_t$ and the viscosity ratio μ_g/μ_o for pressures from the gas dewpoint (CVD pressure) down to a “minimum” pressure. These PVT quantities are used in Eq. 1 to calculate $k_{rg}/k_{ro}(p)$.

The CVD pressures should cover the range from initial dewpoint to the expected abandonment reservoir pressure. The minimum CCE pressure should be selected to represent the lowest BHFP expected (when the well is on decline towards the end of depletion).

Fig. 12 shows an example plot of $k_{rg}/k_{ro}(p)$. The range of “relevant” k_{rg}/k_{ro} is more-or-less given by the k_{rg}/k_{ro} values near the minimum BHFP (marked with closed circles). For this lean gas condensate, the range of k_{rg}/k_{ro} is from about 5 to 50 during the entire life of the well. Typically the relevant range of k_{rg}/k_{ro} is about 1 to 1-1/2 cycles (e.g. 0.5 to 10 for a rich condensate and 10 to 100 for a very lean condensate).

Immiscible Steady State Measurements

Each *immiscible* k_{rg} data should be measured by flowing a pre-selected reservoir gas (with known k_{rg}/k_{ro}) under steady-state conditions at a core pressure close to the minimum BHFP. When steady-state is achieved the pressure drop is measured, and k_{rg} is calculated from the gas flow rate, pressure drop, and gas viscosity; k_{ro} is calculated from $k_{ro}=k_{rg}/(k_{rg}/k_{ro})$.

Steady-state flow can be achieved either by flowing the reservoir (CVD) gas through a back-pressure regulator upstream to the core, thereby lowering the pressure to a value close to the minimum BHFP; else it can be measured by equilibrating the reservoir gas at core pressure and injecting the equilibrium gas and oil at rates that ensure the correct k_{rg}/k_{ro} value given by Eq. 1 [noting $q_o/(q_g+q_o)=V_{roCCE}(P_{core})$].

The five immiscible data should be selected using five flowing mixtures (e.g. CVD gases) that provide more-or-less evenly-spaced k_{rg}/k_{ro} values in the range of interest.

High Capillary Number Measurements

Based on the maximum expected (plateau) rates for a given field using the initial reservoir fluid, the flow velocities can be estimated at the minimum BHFP. At these conditions, a capillary number can be calculated. This capillary number can be used in our correlation for f_1 (Eqs. 20-22) giving the expected improvement in k_{rg} from Eq. 18.

As an example, consider a field with $q_{gmax}=2 \times 10^6$ Sm³/d, $h=100$ m, $r=1$ m, $\phi=0.2$, $S_w=0.25$, $B_{gd}(100 \text{ bara})=0.0125$, $\mu_g=0.02$ mPa-s, $v_g=0.03$ m/s [$v_g=q_{gmax}B_{gd}(pwf)/(2\pi rh\phi(1-S_w))$]. With a gas-oil IFT of $\sigma_{go}=3$ mN/m at 100 bara, $N_c=v_g\mu_g/\sigma_{go}=2 \times 10^{-4}$. For a permeability of $k=50$ md, Eq. 22 estimates $\alpha^o=10^4/[(50)(0.2)]^{0.5}=3160$. For a $k_{rg}/k_{ro}=1$ (a rich gas), $k_{rgI}=0.1$ and $k_{rgM}=0.5$, with $\alpha=(3160)/[(0.1+0.5)/2]=10500$.

The immiscibility factor f_1 at these conditions is $f_1=1/(1+[(10500)(2 \times 10^{-4})]^{0.65})=0.38$, which is a significant improvement in $k_{rg}=0.38(0.1)+(1-0.38)(0.5)=0.35$ (compared with $k_{rgI}=0.1$).

Steady-state measurements (at minimum BHFP) can be made at high flow velocities in the laboratory to achieve higher capillary numbers. However, this has two disadvantages: (1) maximum laboratory pump rates do not usually allow reaching N_c values close to field values, and (2) even if field velocities could be reached, the effect of “inertial” HVF pressure drop may become significant and confuse the interpretation of k_{rg} measurements.

Alternatively, we suggest measuring steady-state flow at higher core pressures with lower gas-oil IFTs. Higher flow velocities can still be used to reach high (near-field) capillary numbers, but it should first be established (e.g. with single-phase gas flow tests) that inertial HVF effects do not occur at these velocities.

k_{rg} should be measured at several velocities for each flowing mixture, and measurements can be repeated at a number of core flowing pressures (i.e. IFT values). To accurately correlate the capillary number, a few IFT measurements may be necessary to tune the IFT correlation (parachors); this is particularly true if $\sigma_{og} < 0.1$ mN/m, where the parachor correlation can be rather inaccurate.

Selecting a Synthetic Gas Mixture

We have found that the same $k_{rg}=f(k_{rg}/k_{ro})$ relation exists for actual reservoir gas condensate and synthetic gas condensate selected to mimic the key PVT behavior of the actual reservoir fluid system. The selection of a synthetic gas can be chosen using pure hydrocarbon compounds (e.g. C₁-C₈-C₁₆), where the molar quantities of the synthetic mixture are determined (automatically by regression) to match the approximate dewpoint, V_{ro} , and Z-factor behavior of the reservoir gas. It is also helpful if the gas-oil viscosity ratio is reasonably close to the reservoir fluid system (at pressures below the dewpoint). **Fig. 13** shows two examples of synthetic gas V_{ro} behavior compared with reservoir fluid CCE liquid dropout curves.

There is some evidence (e.g. the data of Ham and Eilerts¹¹) that the steady-state $k_{rg}=f(k_{rg}/k_{ro})$ behavior is independent of the fluid system (see **Fig. 6**). Additional research is necessary to verify this supposition, but clearly it would make the measurement of *immiscible* k_{rgI} data much simpler. Still, to measure the capillary number dependence of the $k_{rg}=f(k_{rg}/k_{ro})$ relation, synthetic systems with low IFTs must be used.

Fitting Relative Permeability Data

Our procedure for fitting measured relative permeability data correlates $k_{rg}=f(k_{rg}/k_{ro}, N_c)$ using an immiscible equation for k_{rgI} (Arco, Corey, or Chiriaci), and the proposed correlation for capillary number dependence. Exponents and end-point saturations can be modified in the immiscible correlations, while the N_c correlation has only two adjustable parameters, α and n . See Table 1 for an example of the calculations and procedures used in our fitting procedure.

Figs. 14 show an example fit of measured data for a Berea

core and a medium-rich fluid system flowing with a $k_{rg}/k_{ro}=2-3$ for a wide range of capillary numbers (velocities and core pressures). The closed circles are measurements using the reservoir gas condensate system, and the open circles are measurements using the “best-fit” synthetic gas mixture. Gas-oil IFTs for the synthetic gas were in the range 0.8-1.6 mN/m, while for the reservoir gas the estimated IFT was 6.3 mN/m. The proposed correlation is shown as the solid line.

Figs. 15-16 show the results of our proposed relative permeability model used to fit data measured by Marathon⁶ for a near-critical North Sea gas condensate. The open circles are low-pressure laboratory unsteady-state measurements from seven different cores. The solid symbols are measured data using a stack of reservoir cores, flowing initial reservoir gas through the core-stack using a steady-state procedure at varying core pressures. The reservoir-condition data had varying gas-oil IFTs (0.026-0.54 mN/m) and capillary numbers ($2.2 \times 10^{-4} - 7.8 \times 10^{-6}$). The overall fit is shown in **Fig. 16**, indicating that all data are correlated within about 15%.

If saturation data are available, they also can be used in the model parameter fit. However, the only situation we have found where saturation dependence of k_{rg} is important is when the oil saturation in Region 2 (accumulation region outside the condensate blockage zone) reaches values of 15-30%. This is only experienced by medium to rich gas condensates, and even then the effect is second order to the primary k_{rg} reduction in the near-well region.

For gas reservoirs experiencing significant water encroachment, the measurement of trapped gas saturation is important. In gas condensate reservoirs, the trapped gas saturation should be measured first, and “fixed” in the immiscible k_r correlations – i.e., not used as a parameter to fit steady-state k_{rg} data.

Relative Permeability Scaling in Full-Field Models

The different rock types in a full-field simulation model must be assigned consistent relative permeability data. The best modeling approach is to develop a relative permeability correlation that is general for all rock types, or to develop separate correlations for each rock type that exhibits considerably different relative permeability behavior [$k_{rg}=f(k_{rg}/k_{ro})$ behavior]. However, this approach requires a large number of measured data (for each rock type) – data which are usually not available.

When only *limited* relative permeability data are available, end-point scaling can be used to generate relative permeability for different rock types. Our procedure for endpoint scaling of relative permeability uses the *same* scaling for both gas (k_{rg}) and oil relative permeability (to gas, $k_{ro,g}$) curves. For a reference set of relative permeability curves,

$$k_{rg}^{ref} = f(S_g^{ref}, S_{wi}^{ref}, S_{gc}^{ref}, S_{oc}^{ref}) \dots\dots\dots (23)$$

$$k_{ro}^{ref} = f(S_g^{ref}, S_{wi}^{ref}, S_{gc}^{ref}, S_{oc}^{ref}) \dots\dots\dots (24)$$

$$S_g = S_{gc} \frac{S_g^{ref}}{S_{gc}^{ref}}; S_g \leq S_{gc} \dots\dots\dots (25)$$

$$S_g = S_{gc} + \frac{(1 - S_{wi} - S_{oc} - S_{gc})}{(1 - S_{wi}^{ref} - S_{oc}^{ref} - S_{gc}^{ref})} (S_g^{ref} - S_{gc}^{ref});$$

$$S_{gc} < S_g \leq 1 - S_{wi} - S_{oc} \dots\dots\dots (26)$$

$$S_g = 1 + S_{wi} + S_{oc} + \frac{S_{oc}}{S_{oc}^{ref}} (S_g^{ref} - 1 - S_{wi}^{ref} - S_{oc}^{ref});$$

$$1 - S_{wi} - S_{oc} < S_g \leq 1 - S_{wi} \dots\dots\dots (27)$$

$$S_g = 1 - S_{wi} + \frac{S_{wi}}{S_{wi}^{ref}} (S_g^{ref} - 1 + S_{wi}^{ref});$$

$$1 - S_{wi} < S_g \leq 1 \dots\dots\dots (28)$$

The relative permeabilities are scaled with the ratio:

$$k_{rg}(S_g) = k_{rg}^{ref}(S_g^{ref}) \cdot k_{rg}(S_{wi}) / k_{rg}(S_{wi}^{ref}) \dots\dots\dots (29)$$

$$k_{ro}(S_g) = k_{ro}^{ref}(S_g^{ref}) \cdot k_{ro}(S_{wi}) / k_{ro}(S_{wi}^{ref}) \dots\dots\dots (30)$$

This endpoint scaling procedure ensures a reasonable $k_{rg}(k_{rg}/k_{ro})$ relationship for a wide range of endpoints. We have even found that the procedure gives similar results for reservoirs where sufficient data were available to develop independent correlations for each rock type.

Inertial High-Velocity Flow (“Turbulence”)

To quantify the effect of inertial HVF pressure loss, an “effective” gas relative permeability k_{rgHVF} is defined. k_{rgHVF} is defined such that the pressure drop using only Darcy’s law with k_{rgHVF} is equal to the pressure drop using the Forchheimer equation which includes inertial HVF effects. Starting with a single-phase relation for the inertial HVF coefficient β ,

$$\beta = a k^b \phi^c \dots\dots\dots (31)$$

it should be noted that various references give a wide range in constants: $a \sim 10^9 - 10^{10}$, $b \sim 0.5 - 1.5$, and $c \sim 0 - 5.5$. A number of authors have also treated the correction of β for relative permeability effect (see Ref. 3 for a review), where we use the relation

$$\beta_{eff} = \beta \cdot k_{rg}^{-b'} \dots\dots\dots (32)$$

with $b'=b$ taken from the relation in Eq. 31. The choice of correlation for β can have a profound affect on the magnitude of inertial HVF and the effect of relative permeability on β_{eff} (using Eq. 32). In the examples presented below, we use $a=9 \times 10^9$, $b=b'=1$, and $c=0.75$.

Our suggestion is to use an effective gas relative permeability corrected for high velocity effect k_{rgHVF} , defined

as

$$\frac{k_{rgHVF}}{k_{rg}} = \left[1 + \frac{k \cdot k_{rg}}{\mu_g} \cdot \beta_{eff} \cdot \rho_g \cdot v_g \right]^{-1} \dots\dots\dots (33)$$

Effective oil relative permeability including the effect of HVF is calculated by dividing k_{rgHVF} by k_{rg}/k_{ro} .

Velocity Dependence in Pseudopressure

It is necessary to find an approximation that gives velocity as a function of pressure so that capillary number and inertial HVF effects can be included in the pseudopressure function. Our approach is outlined here for radial flow, with similar equations used for linear flow in vertically-fractured wells. For single-phase Darcy flow the velocity in a radial (cylindrical) geometry is given by

$$v(r) = \frac{qB}{2\pi hr} \dots\dots\dots (34)$$

with the steady-state rate equation for pressure p at an arbitrary radius r ,

$$q = \frac{2\pi kh}{\mu B \ln(r/r_w)} (p - p_{wf}) \dots\dots\dots (35)$$

$$p(r) = p_{wf} + \frac{q\mu B}{2\pi kh} \ln(r/r_w) \dots\dots\dots (36)$$

$$r(p) = r_w \exp \left[\frac{2\pi kh}{q\mu B} (p - p_{wf}) \right] \dots\dots\dots (37)$$

where p_{wf} is the wellbore pressure at radius r_w . Radius r in the velocity equation can now be expressed in terms of pressure only, yielding

$$v(p) = \frac{qB}{2\pi h r_w} \exp \left[- \frac{2\pi kh}{q\mu B} (p - p_{wf}) \right] \dots\dots\dots (38)$$

Knowing velocity v as a function of pressure, capillary number is also given in terms of pressure, and the pseudopressure function can be evaluated including capillary number dependence of relative permeabilities. Knowing k_{rg} , the correction to include inertial HVF can be calculated using Eq. 32, where k_{rgHVF} should then be used in the final pseudopressure calculation.

Eq. 35 can be refined using the pseudopressure itself (following single-phase flow analogy as originally proposed for dry gas by Al Hussainy et al.¹),

$$p_p(p(r)) = p_p(p_w) + \frac{q}{2\pi kh} \ln r/r_w \dots\dots\dots (39)$$

The equations above can readily be extended to linear flow for vertically-fractured wells.

An example is presented using the pseudopressure method for calculating reservoir well performance of a rich gas condensate with two well configurations (radial and vertically-fractured). **Figs. 17-22** present results of the calculations.

Figs. 17-18 show the rate-time performance for three assumptions: (a) no N_c dependence on $k_{rg}=f(k_{rg}/k_{ro})$, (b) N_c dependence included using our proposed correlation, Eqs. 18 and 20-22, and (c) both N_c dependence and inertial HVF effects included. For this example, the capillary number dependence has a significant impact on rate-time predictions, while the inertial HVF effect has only a second-order effect.

Looking at the radial well calculations in more detail, **Figs. 19-22** show the pressure dependence of gas pore velocity, capillary number, gas relative permeability, and total mobility. These figures show quantitatively how the capillary number and inertial HVF affect relative permeability and total mobility. It seems clear that the capillary number dependence can be an important factor in predicting reservoir well performance (i.e. condensate blockage) and, consequently, should be measured in the laboratory and correlated for model calculations.

Though the effect of inertial HVF was not particularly important in this example we have found a number of field case histories where inertial HVF in a vertical fracture (or in perforations²²) has had a major impact on the well deliverability. Considerable uncertainty in prediction of β and its dependence on relative permeability exists with today's correlations – more than one order of magnitude. Consequently we recommend that additional measurements be made to improve our quantitative prediction of inertial HVF in gas condensate systems.

Conclusions

1. The oil saturation history experienced in the near-well region of a gas condensate well consists of an unlimited number of cycles of complete or partial drainage and imbibition.
2. Based on our steady-state measurements of several gas condensate systems we have found that the effect of saturation hysteresis is minimal on the fundamental relative permeability relation $k_{rg}=f(k_{rg}/k_{ro})$.
3. Our relative permeability measurements are conducted using a closed-loop apparatus designed specifically to model near-well flow in gas condensate reservoirs, using either synthetic-model or actual gas-condensate reservoir fluids.
4. A design procedure is proposed for defining the laboratory conditions and flowing mixtures that will ensure measurement of relative permeability behavior at relevant flow conditions for the near-well region dictating condensate blockage.
5. Measurements in the closed-loop system can achieve very high capillary numbers using a booster pump system with rates up to 1 liter per minute at elevated core pressures used to reduce gas/oil IFT.
6. A relative permeability model is proposed for fitting steady-state gas/oil relative permeability behavior, including the effect of capillary number on $k_{rg}=f(k_{rg}/k_{ro})$.
7. The effect of capillary number on gas/oil relative permeability can result in a significant improvement in

gas relative permeability and thereby reduce the negative impact of condensate blockage.

8. An empirical but consistent model is proposed for scaling gas/oil relative permeabilities for different rock types and regions with varying end-point saturations. The scaling is applied consistently to the gas and oil relative permeabilities to ensure that the reference (measured) $k_{rg}=f(k_{rg}/k_{ro})$ relation is honored.
9. An approach is given for incorporating (a) the improvement in k_{rg} at high capillary numbers, and (b) the detrimental effect of inertial high velocity flow ("turbulence") as part of the two-phase condensate pseudopressure model. The key to this approach is estimating velocity as a function of pressure in the reservoir using an appropriate form of Darcy's law for the well-flow geometry.

Nomenclature

A	= cross-sectional area to flow; constant in Chierici k_{ro} correlation
B	= constant in Chierici k_{rg} correlation
B_{gd}	= dry-gas FVF
c_{g1}, c_{g2}, c_{g3}	= constants in Arco k_{rg} correlation
c_{o1}, c_{o2}, c_{o3}	= constants in Arco k_{ro} correlation
C_1, C_2	= constants in α correlation
f_I	= immiscibility factor
k	= absolute water permeability, md
k_r	= relative permeability, relative to <i>absolute</i> permeability
k_{rg}	= relative permeability to gas
k_{rgI}	= "immiscible" ($N_c=0$) relative permeability to gas
k_{rgM}	= "miscible" ($N_c=\infty$) relative permeability to gas
k_{rg}^o	= gas relative permeability at S_{wi}
\bar{k}_{rg}	= average gas relative permeability of immiscible and miscible value at $\alpha N_c=1$
k_{ro}	= relative permeability to oil
k_{ro}^o	= oil relative permeability at S_{wi}
k_{rg}/k_{ro}	= gas-oil relative permeability ratio
ΔL	= "characteristic pore-scale length"
L	= core length; constant in Chierici correlation
M	= constant in Chierici correlation
n	= exponent in equation for immiscibility factor
n_g	= exponent in equation for k_{rg} immiscibility factor
n_o	= exponent in equation for k_{ro} immiscibility factor
N_c	= approximate capillary number, $N_c=\Delta p_{viscous}/P_c$
\tilde{N}_c	= "rigorous" capillary number, $=\Delta p_{viscous}/P_c$
N_{cg}	= approximate (gas) capillary number = $v_{pg}\mu_g/\sigma_{go}$
p	= pressure
p_p	= pseudopressure
p_v	= viscous (Darcy) pressure drop
p_{vg}	= gas viscous pressure drop
p_{vo}	= oil viscous pressure drop
Δp	= pressure drop

P_c	= capillary pressure
PV_{inj}	= pore volumes injected
q	= rate
q_g	= core gas rate
q_{inj}	= injection rate evaluated at the pressure of the injection pump
r	= radius
r_{ref}	= reference $k_r(S)$ curve
r_w	= wellbore radius
R_g	= gas saturation variable
R_o	= oil saturation variable
S	= saturation
S_g	= gas saturation
S_{gc}	= critical oil saturation
S_{ge}	= effective gas saturation
S_o	= oil saturation
S_{oc}	= critical (residual-to-gas) oil saturation
S_{oe}	= effective oil saturation
S_w	= water saturation
S_{wi}	= irreducible water saturation
v	= velocity
v_g	= Darcy gas velocity, $v_g = q_g/A$
v_p	= pore velocity, $v_p = q/A\phi(1-S_w)$
v_{pg}	= gas pore velocity
v_{pt}	= total (gas+oil) pore velocity
V_d	= gas volume at dewpoint
V_o	= oil volume
V_{rt}	= V_t/V_d relative volume
V_{ro}	= V_o/V_t relative volume
V_t	= total gas+oil volume at core pressure
Z	= gas Z-factor
α	= scaling parameter for N_c
α^o	= scaling constant for N_c
α_g	= gas scaling parameter for N_c
α_o	= oil scaling parameter for N_c
β	= inertial HVF coefficient
$\beta_{\epsilon\phi\phi}$	= effective inertial HVF coefficient including effect of k_{rg}
λ	= mobility
λ_g	= gas mobility
λ_o	= oil mobility
ρ_g	= gas density
μ_g	= gas viscosity
μ_o	= oil viscosity
σ_{go}	= interfacial tension (IFT)
ϕ	= porosity

Acknowledgements

We want to thank the participants of the "Gas Condensate Well Performance" project – BP, Chevron, INA, Mobil, Norsk Hydro, Norwegian Research Council (NFR), Norwegian Petroleum Directorate (NPD), Occidental International, and Saga Petroleum – for financial and technical support during the two years this work was conducted (1996-1998). We also would like to thank Kameshwar Singh for his assistance.

References

1. Al-Hussainy, R., Ramey, H.J. Jr., and Crawford, P.B.: "The Flow of Real Gases Through Porous Media," *JPT* (May 1966) 624; *Trans., AIME*, **237**.
2. Blom, S.M.P. and Hagoort, J.: "Relative Permeability at Near-Critical Conditions," paper SPE 38935.
3. Blom, S.M.P. and Hagoort, J.: "The Combined Effect of Near-Critical Relative Permeability and Non-Darcy Flow on Well Impairment by Condensate Drop-Out", paper SPE 39976.
4. Blom, S.M.P.: *Relative Permeability to Near-Miscible Fluids*, PhD thesis, Delft U., 1999.
5. Brooks, R.H. and Corey, A.T.: "Properties of Porous Media Affecting Fluid Flow," *J. of the Irrigation and Drainage Division, Proc. of ASCE*, **92**, No. IR2, (1966) 61–88.
6. Chen, H.L., Wilson, S.D., and Monger-McClure, T.G.: "Determination of Relative Permeability and Recovery for North Sea Gas-Condensate Reservoirs," *SPE* (Aug. 1999)393-402.
7. Chierici, G.L.: "Novel Relation for Drainage and Imbibition Relative Permeabilities," *SPEJ* (1984) 275-276.
8. Coats, K.H.: "An Equation of State Compositional Model," *SPEJ* (Oct. 1980) 363-376.
9. Evinger, H.H. and Muskat, M.: "Calculation of Theoretical Productivity Factor," *Trans., AIME* (1942) 146, 126-139.
10. Fevang, Ø. and Whitson, C.H.: "Modeling Gas-Condensate Well Deliverability," *SPE* (Nov. 1996).
11. Ham, J.D. and Eilerts, C.K.: "Effect of Saturation on Mobility of Low Liquid-Vapor Ratio Fluids," *SPEJ* (1967) 11-19.
12. Henderson, G.D., Danesh A., Teherani, D.H., Al-Shaidi, S. and Peden, J.M.: "Measurement and Correlation of Gas Condensate Relative Permeability by the Steady-State Method," *SPEJ*, 1(2), 191-201 (1995).
13. Henderson, G.D., Danesh, A., Tehrani, D., and Peden, J.M.: "The Effect of Velocity and Interfacial Tension on the Relative Permeability of Gas Condensate Fluids in the Wellbore Region," 8th European IOR Symposium (May 15-17, 1995), Vienna.
14. Janicek, J.D. and Katz, D.L.: "Applications of Unsteady State Gas Flow Calculations," in reprint from the U. Michigan Research Conference (June 1955).
15. Jerauld, G.R.: "General Three-Phase Relative Permeability Model for Prudoe Bay," *SPE* (Nov. 1997) 255-263.
16. Jones, J.R. and Raghavan, R.: "Interpretation of Flowing Well Response in Gas Condensate Wells," paper SPE 14204 presented at the 1985 SPE Annual Technical Conference and Exhibition, Las Vegas, Sept. 22-25.
17. Jones, J.R., Vo, D.T., and Raghavan, R.: "Interpretation of Pressure Buildup Responses in Gas Condensate Wells," paper SPE 15535 presented at the 1986 SPE Annual Technical Conference and Exhibition, New Orleans, Oct. 5-8.
18. Muskat, M.: *Physical Principles of Oil Production*, McGraw-Hill Book Company, Inc. (1949).
19. Raghavan, R. and Jones, J.: "Depletion Performance of Gas-Condensate Reservoirs," *JPT* (Aug. 1996) 725-731.
20. Saevareid, A., Whitson, C.H., and Fevang, Ø.: "An Engineering Approach to Measuring and Modeling Gas Condensate Relative Permeabilities", paper presented at the 1999 SCA conference held in Golden, CO, Aug. 2-4, 1999.
21. Standing, M.B.: "Notes on Relative Permeability Relationships," *Proc., University of Trondheim, NTH, Norway* (1975).
22. Stewart, George: Personal communication, IBC Conference on Optimisation of Gas Condensate Fields, 1997.
23. Whitson, C.H. and Fevang, Ø.: "Generalized Pseudopressure Well Treatment in Reservoir Simulation," in *Proc. IBC Conference on Optimisation of Gas Condensate Fields*, 1997.

Appendix A – Capillary Number Definition

Developing an expression for "total" capillary number, based on total (gas+oil) viscous forces,

$$\tilde{N}_c \equiv \frac{\Delta p_v}{\Delta p_c} \dots\dots\dots (40)$$

$$\Delta p_v = v_{pt} \frac{\Delta L}{k(k_{rg}/\mu_g + k_{ro}/\mu_o)} \dots\dots\dots (41)$$

$$P_c = \frac{2\sigma_{go}}{r} \approx \frac{C_1\sigma}{\sqrt{k/\phi}}; \bar{r} \propto \sqrt{k/\phi} \dots\dots\dots (42)$$

$$\frac{\Delta p_v}{P_c} = \frac{v_{pt} \Delta L}{\lambda_g + \lambda_o} \frac{k}{C_1\sigma_{go}} \frac{1}{\sqrt{k/\phi}} \dots\dots\dots (43)$$

$$\tilde{N}_{ct} = \frac{v_{pt}}{\sigma_{go}} \frac{\Delta L}{(\lambda_g + \lambda_o) C_1\sqrt{k/\phi}} \dots\dots\dots (44)$$

Defining an equivalent gas-phase capillary number,

$$\Delta P_{vg} = v_{pg} \frac{\Delta L}{k k_{rg}/\mu_g} \dots\dots\dots (45)$$

$$\Delta P_{vo} = v_{po} \frac{\Delta L}{k k_{ro}/\mu_o} \dots\dots\dots (46)$$

$$\tilde{N}_{cg} = \frac{v_{pg}\mu_g}{\sigma_{go}} \frac{\Delta L}{C_1 k_{rg} \sqrt{k/\phi}} = \tilde{N}_{ct} \dots\dots\dots (47)$$

can be expressed in terms of the approximate gas capillary number N_{cg} defined in Eq. 16,

$$\tilde{N}_{cg} = \frac{v_g\mu_g}{\sigma_{go}} \frac{\Delta L}{C_1 k_{rg} \sqrt{k/\phi}} = N_{cg} \alpha \dots\dots\dots (48)$$

$$\alpha_g = \frac{\Delta L}{C_1 k_{rg} \sqrt{k/\phi}} \dots\dots\dots (49)$$

In all equations above the term ΔL is a "characteristic pore-scale length" which we assume is more-or-less constant for most porous media (or can be correlated as a function of some rock property such as permeability or mean pore-size).

Simplified Gas Capillary Number (most common)

$$N_{cg} = \frac{v_{pg}\mu_g}{\sigma_{go}} = \frac{\tilde{N}_{cg}}{\alpha} = \frac{\tilde{N}_{ct}}{\alpha} \dots\dots\dots (50)$$

We note that,

$$\alpha = \frac{C_2}{\bar{k}_{rg} \sqrt{k \phi}} = \frac{\alpha^0}{\bar{k}_{rg}} \dots\dots\dots (51)$$

where α is *not* a constant because of its dependence on $\bar{k}_{rg} = 0.5(k_{rgM} + k_{rgI})$. We define, therefore, a constant α^0 which is only a function of rock properties,

$$\alpha^0 = \frac{C_2}{\sqrt{k \phi}} \dots\dots\dots (52)$$

We found that $C_2=10^4$ (for k in md) gives an excellent fit of the published $k_{rg}=f(k_{rg}/k_{ro})$ data from Heriot-Watt and Delft universities, where our proposed relation (Eq. 18-20) is used with $n=0.65$ and N_{cg} .

We have studied the loss in accuracy when using the approximate gas capillary number N_{cg} instead of the more

rigorous capillary number $\tilde{N}_c (= \tilde{N}_{cg})$. First we assumed (for the sake of argument) an “exact” model with $\alpha=1$ and $n=0.75$ using \tilde{N}_c for correlation of $k_{rg}=f(k_{rg}/k_{ro})$ based on Eq. 18. We then fit the exact model relative permeabilities using the approximate gas capillary number N_{cg} . The result was a near-perfect fit of the exact model, but with n varying slightly with k_{rg}/k_{ro} ; n varied from 0.75 to 0.62 by less than 0.02 per log cycle. Using a constant $n=0.65$ with N_{cg} gives a very good representation of exact-model k_{rg} for k_{rg}/k_{ro} between 0.1 and 100 (the k_{rg}/k_{ro} region of interest for gas condensates).

In conclusion, we see no reason why the approximate gas capillary number definition $N_{cg}=v_{gp}\mu_g/\sigma_{go}$ can not be used for correlating relative permeability data. The most important issue is that a consistent definition be used for capillary number when (a) fitting measured data and (b) applying capillary number dependence in reservoir modeling.

TABLE 1 – EXAMPLE (EXCEL) PROGRAM FOR FITTING IMMISCIBLE AND HIGH N_c RELATIVE PERMEABILITY DATA FOR A NORTH SEA NEAR-CRITICAL GAS CONDENSATE RESERVOIR.

CoreyFit North Sea Near-Critical Gas Condensate Example

A Program for Fitting Gas Condensate (Steady State) Relative Permeability Data to Corey Model
© 1998 Pera a/s

Input Permeability and Porosity	
Permeability, md	20
Porosity, fraction	0.22
Alpha Estimate	4767

Regression-Related Parameters			
Initial	Final	Minimum	Maximum
Alpha	1218.9	1000	10000
n	-0.650	-0.50	-1.00
LambdaC	0.500	0.50	10.00
LambdaC	3.508	0.50	10.00
Swi	0.130	0.00	1.00
Soc	0.150	0.00	0.50
Sm	1.000	0.80	1.20
Sgc	0.000	0.00	0.50

Copy of Initial Parameters
4767.0
-0.650
2.000
2.000
0.130
0.150
1.000
0.000

Swi+Soc	0.280
Somin	0.150 (Kro>0)
Somax	0.870 (Kro>0)
Sgmin	0.000 (Krg>0)
Sgmax	0.720 (Krg>0)

SSQ	1.81E+00
-----	----------

Note: High Nc data at bottom of input data list (106-111)

Data No.	Measured					Model										Krg			
	Input Required and Optional Data					Calc'd	KrgM	S*	So	Sg	KrgI	f	Krg	Kro	Krg.avg	SSQi	wi	% SSQi	SSQi
106	0.45000	0.21200	2.122642	2.23E-04		0.870	0.679758	0.55818	0.4856	0.3844	0.18463	0.57488	0.39512	0.18615	0.43219	1.49E-02	1.0	0.0	0.00E+00
107	0.27600	0.26300	1.04943	6.25E-05		0.870	0.512059	0.61237	0.5328	0.3372	0.13732	0.71960	0.24239	0.23098	0.32469	1.48E-02	1.0	0.0	0.00E+00
108	0.23700	0.25300	0.936759	3.36E-05		0.870	0.483673	0.62107	0.5403	0.3297	0.13032	0.78737	0.20545	0.21933	0.30700	1.77E-02	1.0	0.0	0.00E+00
109	0.15300	0.23900	0.640167	1.59E-05		0.870	0.390306	0.64993	0.5654	0.3046	0.10834	0.84012	0.15342	0.23965	0.24932	7.43E-06	1.0	0.0	0.00E+00
110	0.11900	0.20200	0.589109	1.07E-05		0.870	0.370717	0.65614	0.5708	0.2992	0.10386	0.86859	0.13893	0.23583	0.23729	2.80E-02	1.0	0.0	0.00E+00
111	0.10200	0.19600	0.520408	7.81E-06		0.870	0.342282	0.66536	0.5789	0.2911	0.09738	0.88500	0.12555	0.24125	0.21983	5.33E-02	1.0	0.0	0.00E+00
1	0.15160	0.25372	0.5975	1.00E-10	0.7680	0.102	0.374022	0.65510	0.5699	0.3001	0.10461	0.99992	0.10463	0.17511	0.23931	9.60E-02	1.0	0.0	0.00E+00
2	0.18070	0.19872	0.9093	1.00E-10	0.7370	0.133	0.476248	0.62334	0.5423	0.3277	0.12852	0.99993	0.12855	0.14137	0.30238	8.33E-02	1.0	0.0	0.00E+00
3	0.20250	0.15590	1.2989	1.00E-10	0.7070	0.163	0.565009	0.59598	0.5185	0.3515	0.15096	0.99994	0.15099	0.11624	0.35799	6.47E-02	1.0	0.0	0.00E+00
4	0.21910	0.12665	1.73	1.00E-10	0.6820	0.188	0.633700	0.57390	0.4993	0.3707	0.17026	0.99994	0.17029	0.09843	0.40198	4.96E-02	1.0	0.0	0.00E+00
5	0.23320	0.10471	2.227	1.00E-10	0.6590	0.211	0.690115	0.55450	0.4824	0.3876	0.18807	0.99995	0.18810	0.08446	0.43909	3.74E-02	1.0	0.0	0.00E+00
100	0.36410	0.00822	44.2993	1.00E-10	0.443	0.427	0.977925	0.35365	0.3077	0.5623	0.41545	0.99996	0.41547	0.00938	0.69669	1.99E-02	1.0	0.0	0.00E+00
101	0.39760	0.00513	77.5068	1.00E-10	0.421	0.449	0.987262	0.32529	0.2830	0.5870	0.45357	0.99996	0.45359	0.00585	0.72042	1.98E-02	1.0	0.0	0.00E+00
102	0.43720	0.00282	155.0496	1.00E-10	0.389	0.481	0.993592	0.29463	0.2563	0.6137	0.49644	0.99996	0.49646	0.00320	0.74501	1.84E-02	1.0	0.0	0.00E+00
103	0.46270	0.00149	310.5436	1.00E-10	0.362	0.508	0.996790	0.26870	0.2338	0.6362	0.53405	0.99996	0.53406	0.00172	0.76542	2.38E-02	1.0	0.0	0.00E+00
104	0.48100	0.00078	616.7179	1.00E-10	0.341	0.529	0.998381	0.24745	0.2153	0.6547	0.56581	0.99996	0.56583	0.00092	0.78210	3.11E-02	1.0	0.0	0.00E+00

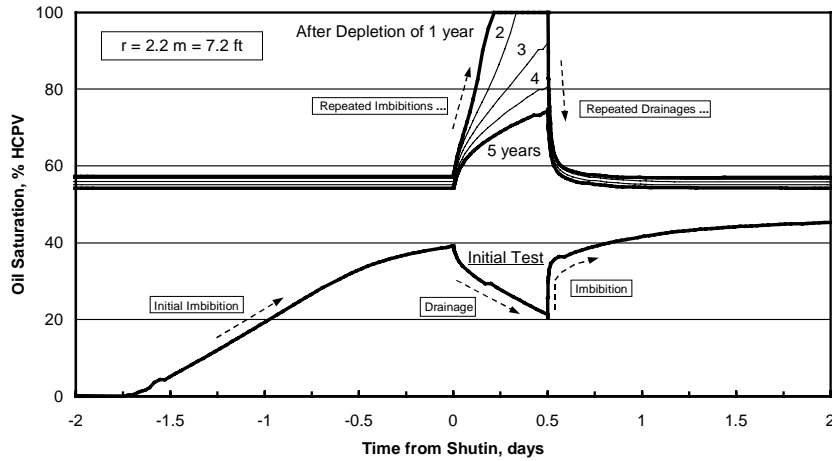


Fig. 1 — Saturation hysteresis prior-to and following the annual 12-hour shutins in a gas condensate well – at a radius 2.2 m from the wellbore. Shows complete and partial cycles of drainage and imbibition.

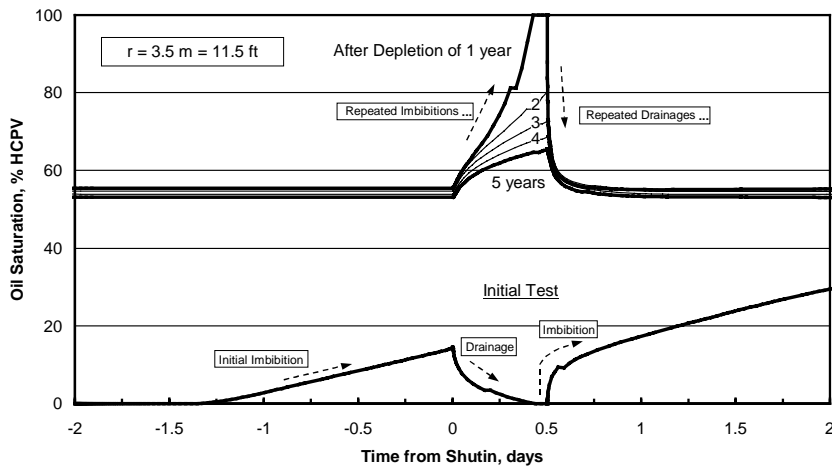


Fig. 2 — Same as Fig. 1 but at a radius 2.2 m from the wellbore.

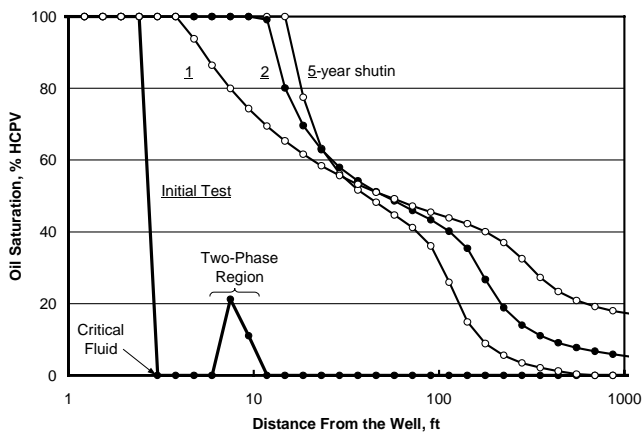


Fig. 3 — Saturation profiles following a 12-hour shutin for a gas condensate well – for a gas condensate well during the first five years of depletion. Shows the development of a solid oil “bank” in the near-well region, as well as complex near-critical and two-phase regions beyond the oil bank.

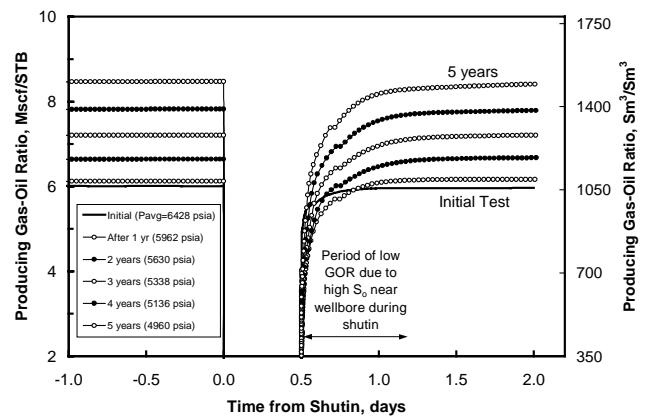


Fig. 4 — Producing GOR variation prior and following the annual 12-hour shutins – for a gas condensate well during the first five years of depletion. Post-shutin GOR behavior shows overly-rich produced wellstream due the “emptying” of the oil bank that develops near the well during the shutin period.

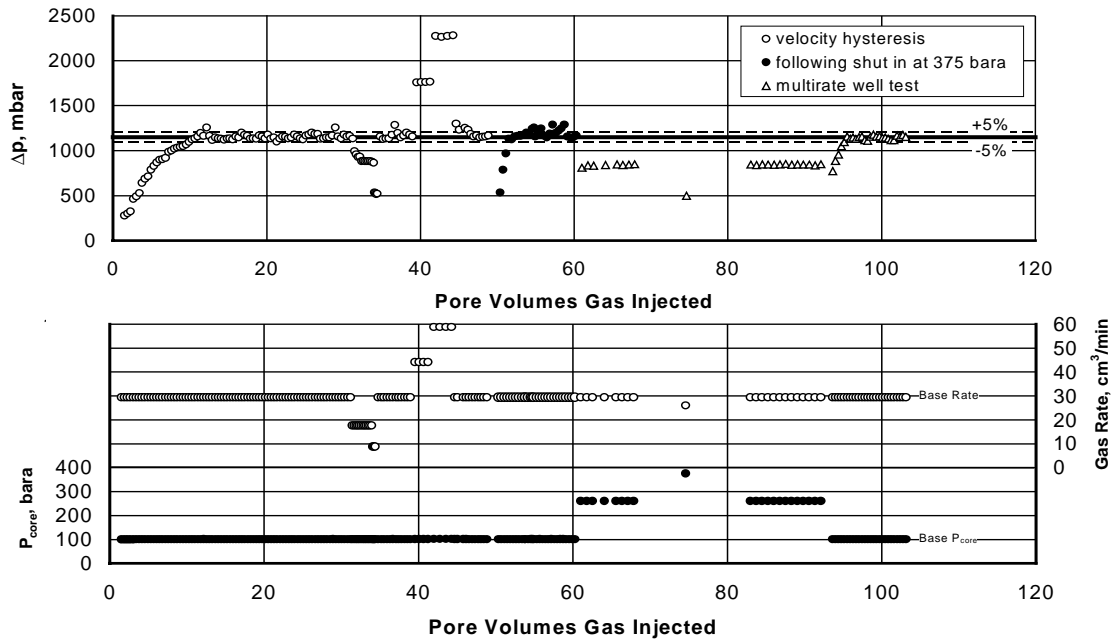


Fig. 5 — Hysteresis test for Berea 1, synthetic gas 1, for rich (synthetic) reservoir gas with $k_{rg}/k_{ro}=0.7$.

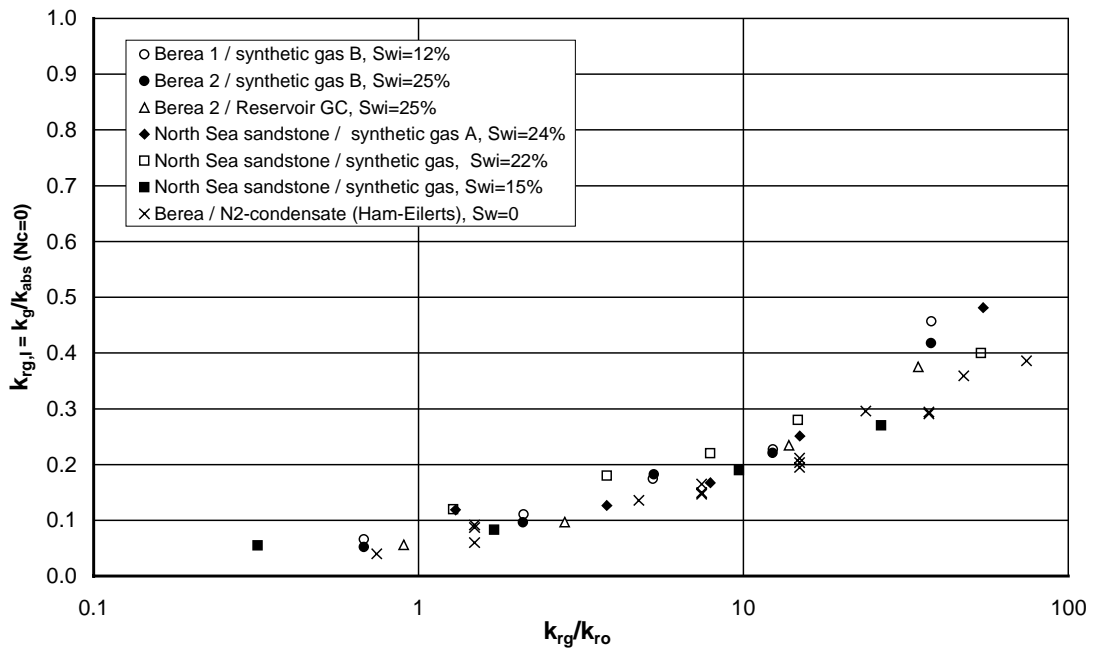


Fig. 6 — Immiscible (low- N_c) relative permeability measurements for two Berea and one North Sea sandstone compared with results for a Berea sample reported by Ham and Eilerts¹¹.

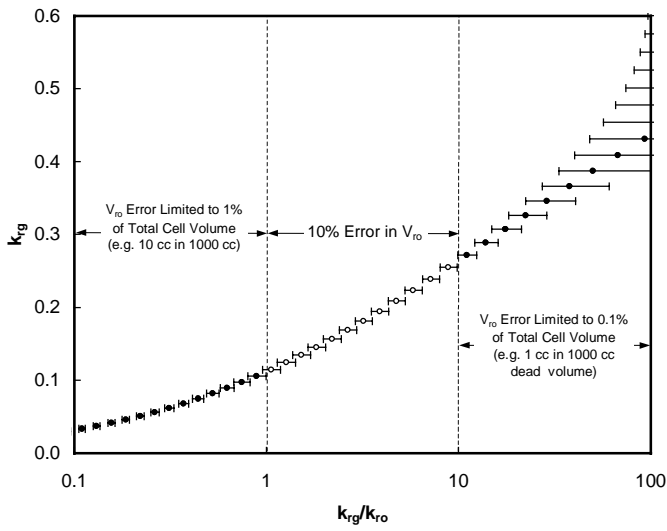


Fig. 7 — A $k_{rg}=f(k_{rg}/k_{ro})$ relation showing the effect of potential (and realistic) errors in V_{ro} when calculating k_{rg}/k_{ro} from Eq. 1.

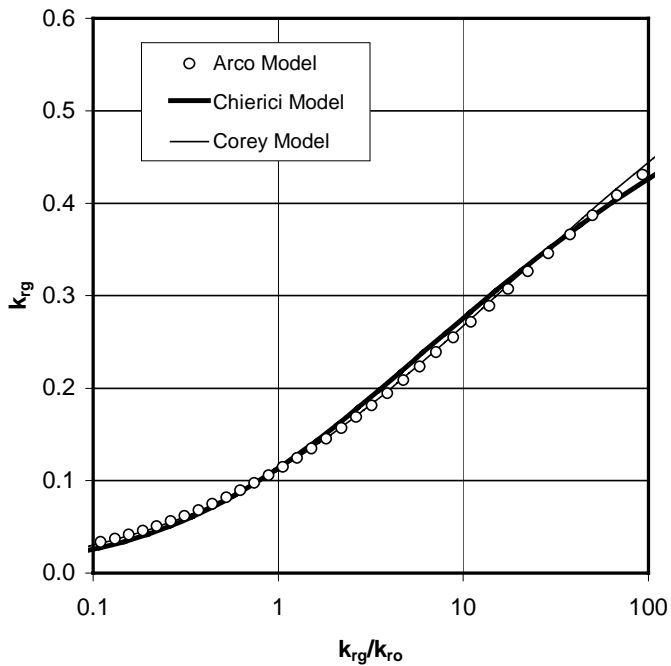


Fig. 8 — Fundamental $k_g=f(k_{rg}/k_{ro})$ relationship using three different immiscible correlations, showing essentially identical behavior in the entire range of k_{rg}/k_{ro} of interest (from very rich to very lean gas condensate systems).

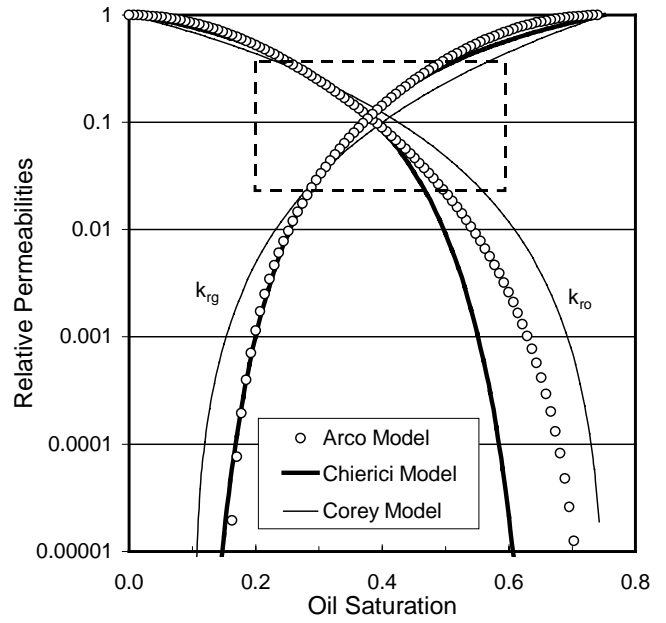


Fig. 9 — Saturation dependent relative permeability curves for three correlations, showing in particular the region of relative permeabilities that affect flow behavior in the near-well region (boxed area). The three correlations have the “same” $k_{rg}=f(k_{rg}/k_{ro})$ relationship in the boxed region.

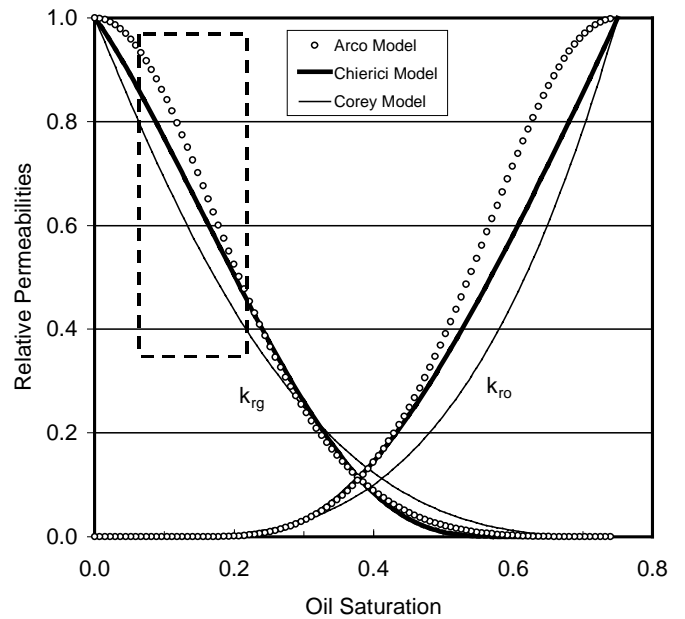


Fig. 10 — Saturation dependent relative permeability relations for three correlations, showing in particular the region of relative permeabilities that affect flow behavior in the “distant” accumulation region away from the well (boxed area). The three correlations have the “same” $k_{rg}=f(k_{rg}/k_{ro})$ relationship.

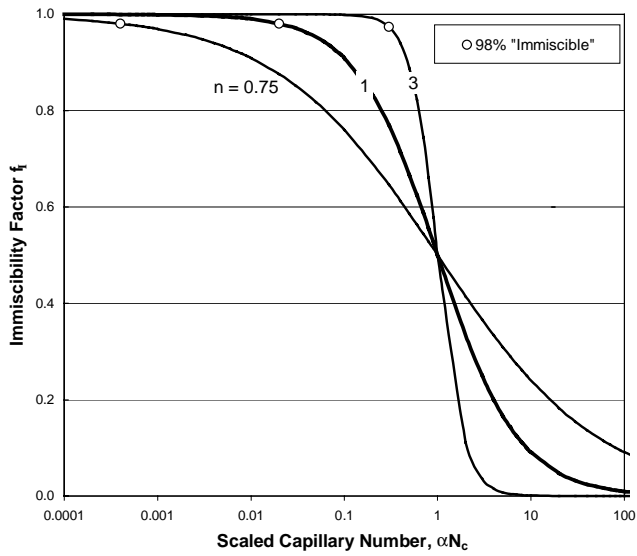


Fig. 11 — Behavior of the immiscibility factor coupling immiscible and miscible relative permeabilities as a function of capillary number. Shows behavior for three values of the exponent n , highlighting the (scaled) capillary number where 98% of the total k_{rg} is due to “immiscible” behavior.

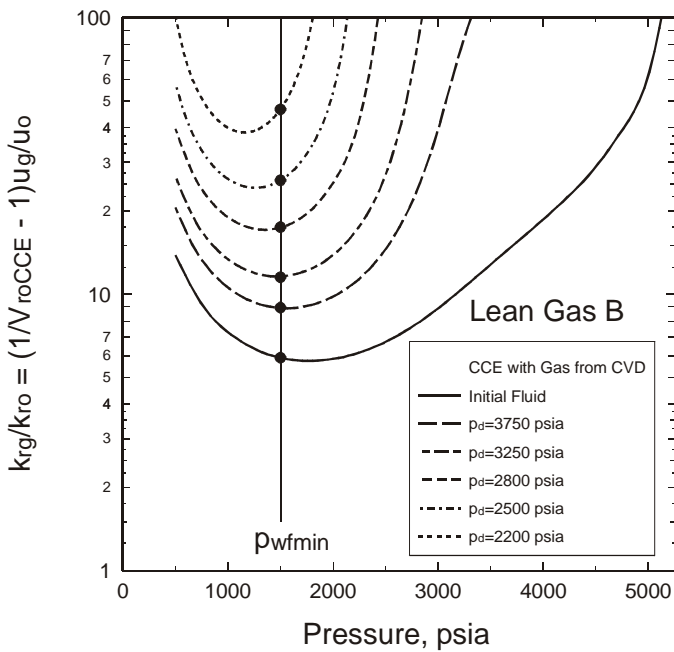


Fig. 12 — Design plot for determining the relevant range of k_{rg}/k_{ro} during depletion of a gas condensate reservoir, where the k_{rg}/k_{ro} values of interest are close to the minimum BHFP.

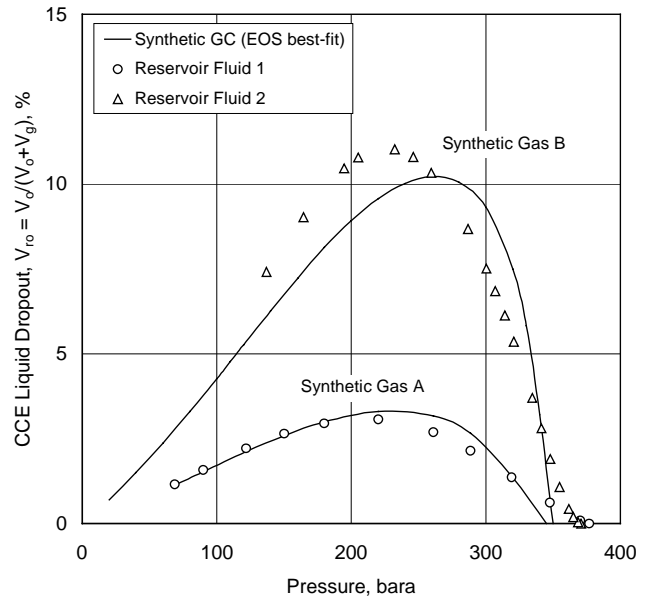


Fig. 13 — Example comparisons of oil relative volume behavior between two reservoir fluids and their synthetic gas “best-fit” mixtures.

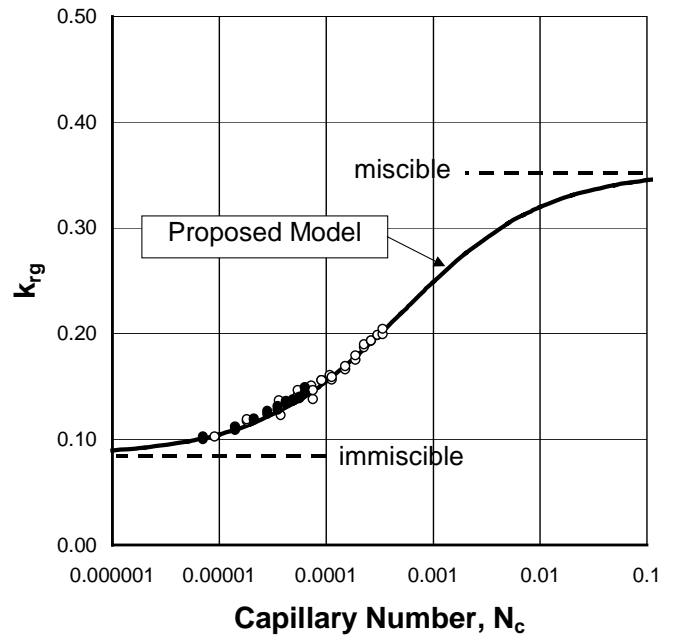


Fig. 14 — Fit of measured k_{rg} data with the proposed relative permeability model for a wide range of capillary numbers and a more-or-less constant $k_{rg}/k_{ro} = 2$.

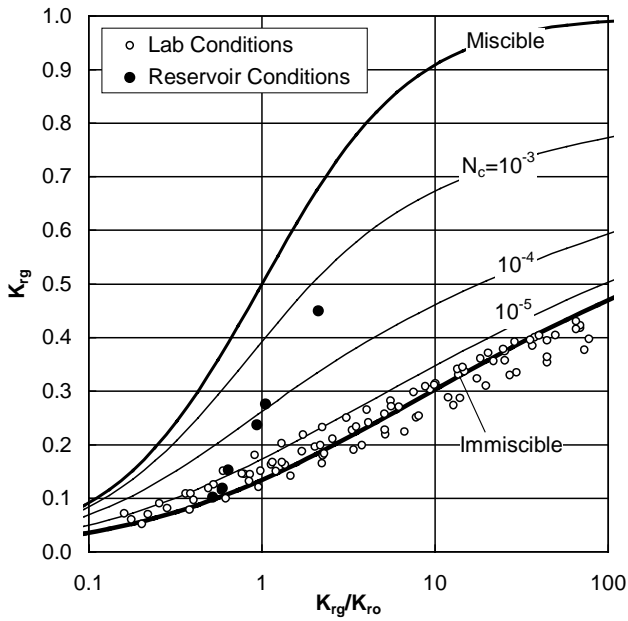


Fig. 16 — Fit of all available k_{rg} data using the proposed relative permeability model .

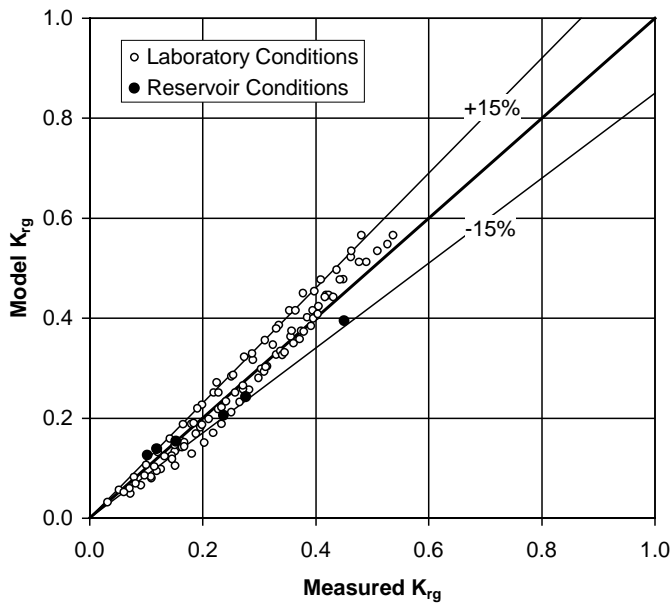


Fig. 17 — Quality of fit to measured relative permeability data from a North Sea rich gas condensate field using proposed model including capillary number dependence of $k_{rg}=f(k_{rg}/k_{ro})$.

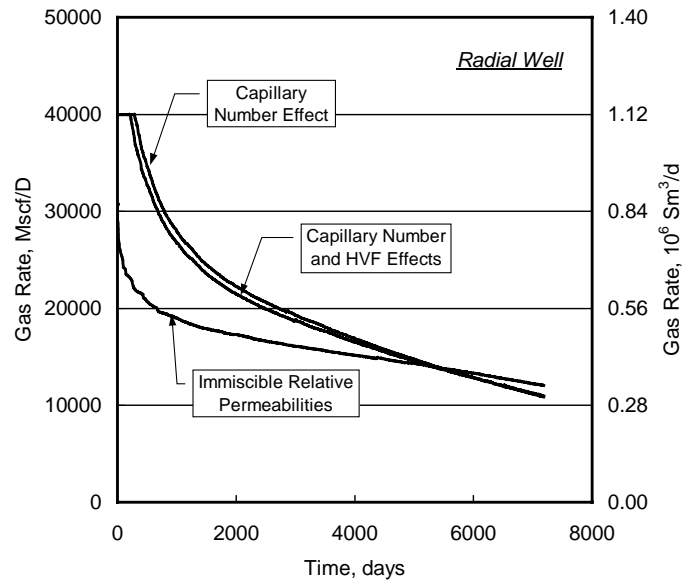


Fig. 18 — Rate-time behavior for a rich gas condensate *radial* well showing the effect of including capillary number improvement of k_{rg} , and inertial high velocity flow (“turbulence”).

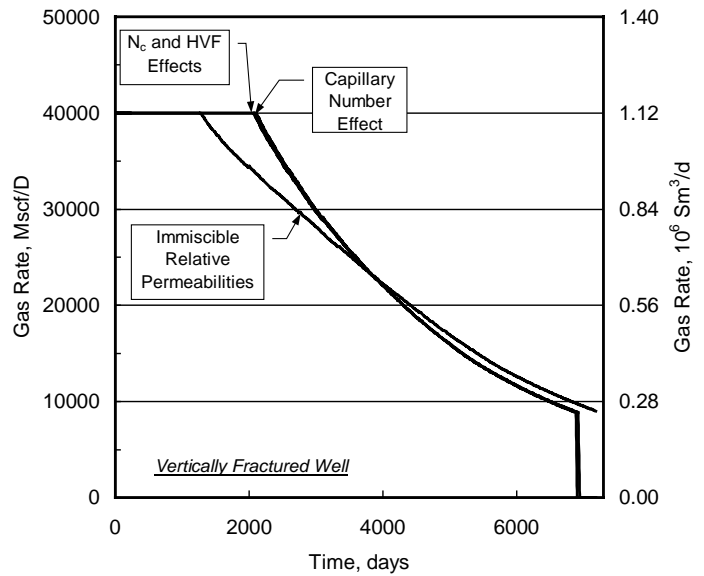


Fig. 19 — Rate-time behavior for a rich gas condensate *vertically-fractured* well showing the effect of including capillary number improvement of k_{rg} , and inertial high velocity flow (“turbulence”).

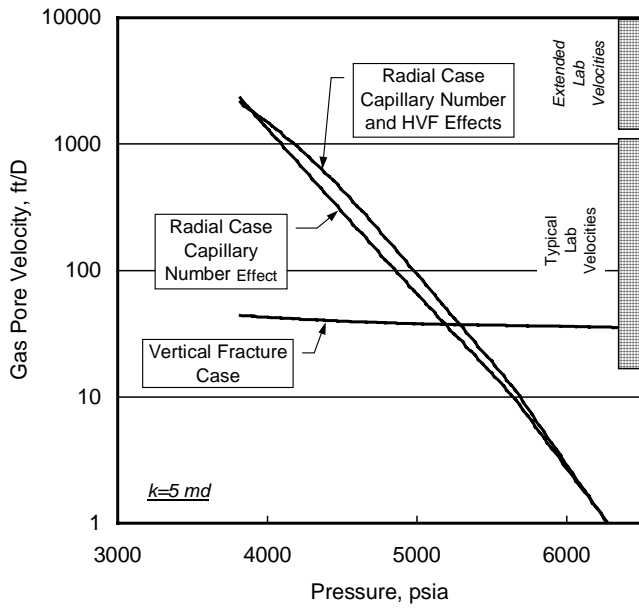


Fig. 20 — Example gas “pore” velocities variation with pressure for radial and vertically-fractured (linear) flow geometries in a rich gas condensate well using proposed steady-state pseudopressure model.

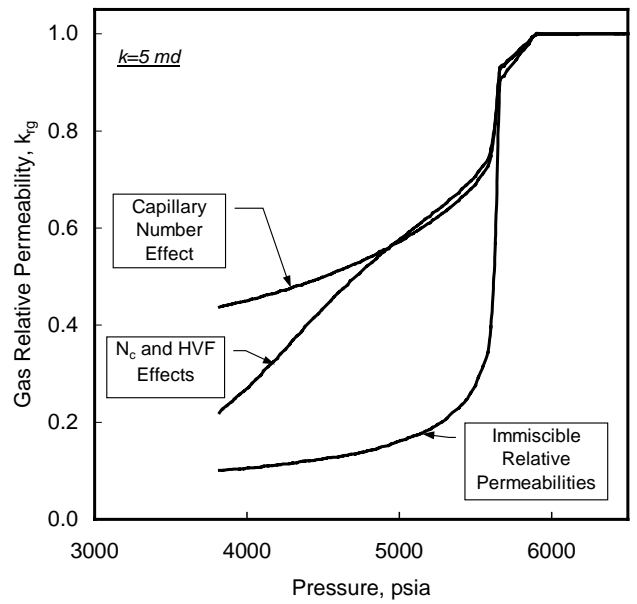


Fig. 22 — Example gas relative permeability variation with pressure for radial flow geometry in a rich gas condensate well using proposed steady-state pseudopressure model; shows effect of N_c dependence on k_{rg} and effect of internal HVF (“turbulence”) on capillary number.

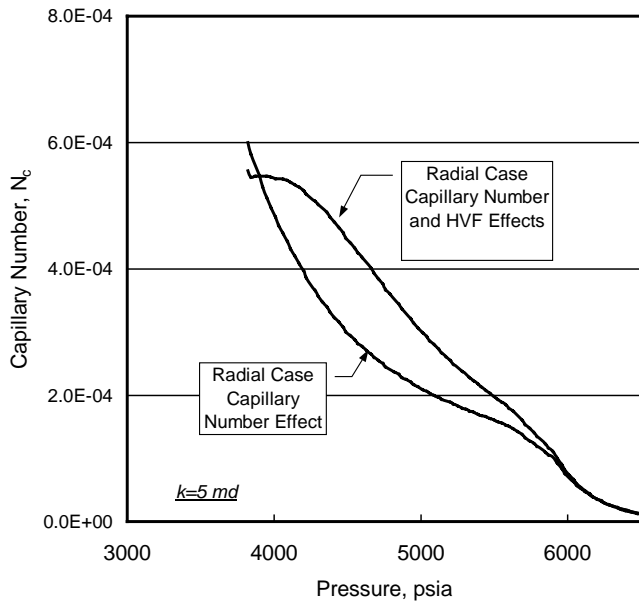


Fig. 21 — Example capillary number variation with pressure for radial flow geometry in a rich gas condensate well using proposed steady-state pseudopressure model; also shows effect of internal HVF (“turbulence”) on capillary number.

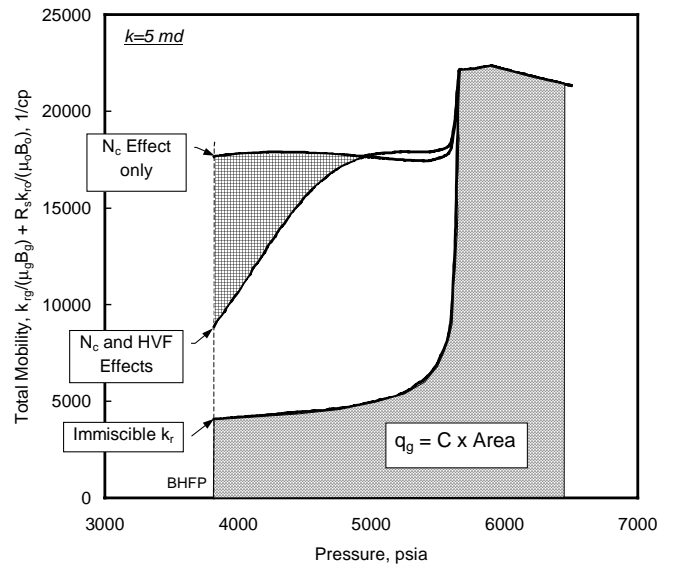


Fig. 23 — Example total mobility (pseudopressure function) variation with pressure for radial flow geometry in a rich gas condensate well using proposed steady-state pseudopressure model; shows effect of N_c dependence on k_{rg} and internal HVF (“turbulence”) on capillary number.